ACS APPLIED POLYMER MATERIALS

pubs.acs.org/acsapm

Article

Poly(aryl cyanurate)-Based Thin-Film Composite Nanofiltration Membranes

Maria G. Elshof, Evelien Maaskant, Mark A. Hempenius, and Nieck E. Benes*

Cite This: *ACS Appl. Polym. Mater.* 2021, 3, 2385−2392

Read Online

ACCESS | Metrics & More | Article Recommendations | Supporting Information

ABSTRACT: The successful synthesis of poly(aryl cyanurate) nanofiltration membranes via the interfacial polymerization reaction between cyanuric chloride and 1,1,1-tris(4-hydroxyphenyl)ethane (TPE), atop a polyethersulfone ultrafiltration support, is demonstrated. The use of cyanuric chloride allows for the formation of a polymer that does not contain hydrolysis-susceptible amide bonds that inherently limit the stability of polyamide nanofiltration membranes. In order to achieve a thin defect-free cross-linked film via interfacial polymerization, a sufficient number of each monomer should react. However, the reactivities of the second and third chloride groups of the cyanuric chloride are moderate. Here, this difficulty is overcome by the high functionality and the high reactivity of TPE.

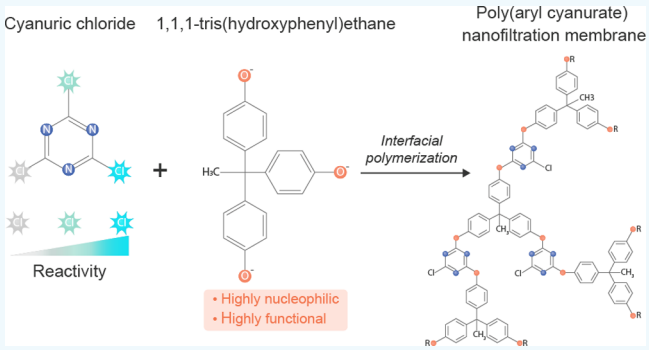

The membranes demonstrate a typical nanofiltration behavior, with a molecular weight cutoff of 400 ± 83 g·mol^{-1} and a permeance of 1.77 ± 0.18 L·m^{-2} h^{-1} bar^{-1}. The following retention behavior Na_2SO_4 (97.1%) > $MgSO_4$ (92.8%) > NaCl (51.3%) > $MgCl_2$ (32.1%) indicates that the membranes have a negative surface charge. The absence of amide bonds in the membranes was expected to result in superior pH stability as compared to polyamide membranes. However, it was found that under extremely acidic conditions (pH = 1), the performance showed a pronounced decline over the course of 2 months. Under extremely alkaline conditions (pH = 13), after 1 month, the performance was lost. After 2 months of exposure to moderate alkaline conditions (pH = 12), the $MgSO_4$ retention decreased by 14% and the permeance increased by 2.5-fold. This degradation was attributed to the hydrolysis of the aryl cyanurate bond that behaves like an ester bond.

KEYWORDS: *NF membrane, poly(aryl cyanurate), interfacial polymerization, thin-film composite, hydrolysis, triazine*

1. INTRODUCTION

Nanofiltration (NF) membranes are useful in many applications, such as decontamination and recycling of industrial wastewater,[1,2] food processing,[3] treatment of textile wastewater,[4−6] and water softening.[7,8] With pore sizes of 0.5−2 nm and a corresponding molecular weight cutoff (MWCO) of 200−1000 g·mol^{-1},[9] NF membranes have separation performances falling in-between those of reverse osmosis and ultrafiltration membranes.[10] They are typically used for the removal of small organic molecules and multivalent ions from liquids.

The application of NF membranes is limited by their chemical stability to processes with moderate operating conditions.[11] Enhancing the chemical stability of nanofiltration membranes will enable potential applications in the chemical industry that involve much more aggressive conditions, such as extreme pH environments (i.e., below pH = 2 and above pH = 12.5). Potential applications include the recovery of acids used in the metal industry,[12] the removal of sulfate ions from mining effluents,[13] and the treatment of effluents generated by the paper industry[14] and the textile industry.[15] Traditional thin-film composite (TFC) polyamide membranes are not stable under extreme pH conditions because they contain ester or amide bonds that are susceptible to hydrolysis.[16] Commercially available NF alternatives have several drawbacks, including being resistant only to acidic pH conditions, being resistant only to mild conditions, having a too high MWCO or low flux, or being expensive.[11] Therefore, recent research has moved toward the development of new types of pH-stable membranes without compromising the flux and selectivity.[11] For example, grafted polyvinylidene fluoride membranes, graphene-incorporated polyethersulfone membranes, sulfonated poly(ether ether ketone)-based membranes on polyethersulfone supports, and polyamide membranes prepared by exchanging the traditional piperazine for 1,3,5-(tris-piperazine)-triazine in the polymer-

Received: December 10, 2020
Accepted: March 30, 2021
Published: April 13, 2021

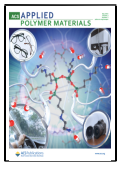

https://doi.org/10.1021/acsapm.0c01366
ACS Appl. Polym. Mater. 2021, 3, 2385−2392

Scheme 1. Formation of a Cross-Linked Poly(aryl cyanurate) Network by the Reaction of TPE with CC[a]

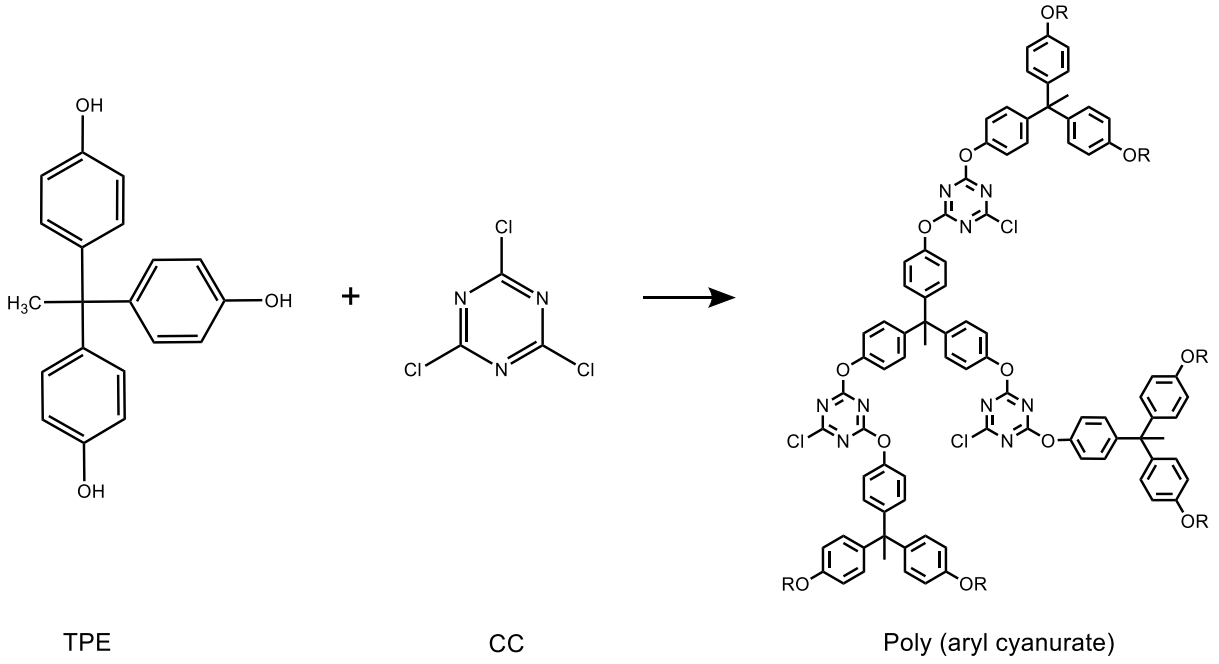

[a]The ether bonds are expected to provide stability under extreme pH conditions.

ization process, among others, have all been investigated for higher pH stability without a loss of performance.[17−20]

A promising new development is the production of polyamine membranes, as shown by Lee et al. (2015). These authors have used cyanuric chloride (CC) instead of traditional acyl chloride in the interfacial polymerization reaction, to produce polyamine membranes that do not contain carbonyl groups and are stable at extreme pH.[11] A drawback of using CC is the limited reactivity of this monomer. By combining CC with several different amines, Lee et al. have demonstrated that thin defect-free membranes can only be obtained when the aqueous phase monomer contains more than two nucleophilic reactive groups.[21] This approach was not successful for the small aromatic amine melamine due to the too low solubility of this monomer. Maaskant[22] demonstrated the successful preparation of potentially pH-stable freestanding aromatic polycyanurate films via an interfacial polycondensation of CC with trifunctional aromatic alcohols. Further building on this chemistry, here we present the preparation and characterization of TFC membranes, comprising a poly(aryl cyanurate) film atop a polyethersulfone ultrafiltration support.

2. EXPERIMENTAL SECTION

2.1. Chemicals and Materials. CC (99%), sodium hydroxide (NaOH, puriss. p.a., ACS reagent ≥98%), sodium chloride (NaCl, ≥99%), sodium dodecyl sulfate (SDS, ACS reagent ≥99.0%), and poly(ethylene glycol) (PEG) with molecular weights of 400, 600, and 1500 g mol^{-1} were obtained from Sigma Aldrich (Germany).

Sodium sulfate (Na_2SO_4, anhydrous, for analysis EMSURE ACS), magnesium sulfate heptahydrate ($MgSO_4$, for analysis EMSURE ACS), and PEG 1000 (EMPROVE ESSENTIAL) were obtained from Merck Millipore (Germany).

Magnesium chloride hexahydrate ($MgCl_2$, 99.0−101.0%, AnalaR NORMAPUR ACS Reag.) was purchased from VWR chemicals (Netherlands). *n*-Hexane (anhydrous, over molecular sieves) was acquired from Alfa Aesar (Germany). 1,1,1-Tris(4-hydroxyphenyl)-ethane (TPE, >98.0%) was acquired from TCI (Belgium). PEG 200 was obtained from Fluka (Germany).

Milli-Q water was used to prepare all aqueous solutions. All chemicals were used as received.

Hydrophilized polyethersulfone (PES) ultrafiltration (UF) membranes with a MWCO of 30 kDa were purchased from Microdyn-Nadir (UH030, Germany) and used as the support. According to the supplier and earlier research, these supports are stable in the pH range 0−14.[11]

2.2. Membrane Preparation. Poly(aryl cyanurate) TFC membranes were fabricated by an interfacial polymerization reaction between TPE and CC on top of a PES support UF membrane. TPE is deprotonated by the use of NaOH. As Cl is an electron-withdrawing group, it has a partial negative charge and the carbon atom has a slightly positive charge. Nucleophilic substitution takes place by attack of the deprotonated TPE on the carbon atom, resulting in the loss of HCl. The resulting structure is shown in Scheme 1.

For the aqueous phase, TPE (1 w/v %) with NaOH (1:3 mole ratio) was dissolved in Milli-Q water. The organic solution was prepared by dissolving 0.01 w/v % CC in anhydrous *n*-hexane.

Preparation of the TFC membranes was performed in the following steps. First, a 7 × 10.5 cm piece of PES support was soaked in 0.05 wt % SDS solution overnight, in order to wet the pores and remove residual surfactant. After this, it was rinsed with water and placed in the IP cell, which was sealed using a Viton O-ring and clamps as shown in Supporting Information, Figure S1. Any residual water drops on the surface were removed by applying a vacuum for a few seconds. Next, 25 mL of aqueous solution was poured on top of the support membrane and left to soak for 5 min. Subsequently, vacuum was applied to pull the aqueous solution through the membrane and obtain a dry surface. Then, 25 mL organic solution was poured on top, and the monomers were left to react for 30 s, followed by discarding the organic solution. Unreacted monomers were washed off by immediately placing the membrane after the reaction step in a hot water bath of ∼45 °C for 5 min. Finally, membranes were stored in Milli-Q water overnight prior to characterization.

It must be noted that the above-mentioned IP conditions were not optimized but were chosen such that the obtained membranes were within the NF regime and the pH stability tests could be performed.

https://doi.org/10.1021/acsapm.0c01366
ACS Appl. Polym. Mater. 2021, 3, 2385−2392

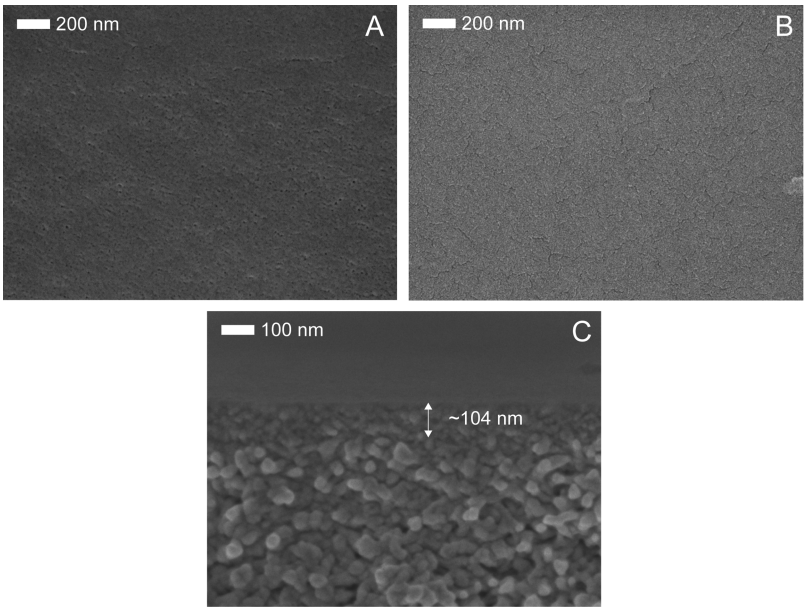

Figure 1. FE-SEM pictures of the PES support (A), TPE-CC TFC membrane surface (B), and cross section (C).

2.3. Characterization. The fabricated membranes were characterized based on their morphology and functional groups, using scanning electron microscopy and Fourier transform infrared spectroscopy (FTIR).

Field emission scanning electron microscopy (FE-SEM, JSM-7610F) was used to observe the surface and cross-sectional morphology of the membranes. Prior to characterization, samples were dried overnight in a vacuum oven at 50 °C. Cross-sectional samples were prepared by cutting the membranes in liquid nitrogen with a sharp blade. To prevent charging, carbon paint was applied on the edges. All samples were sputtered with a 5 nm Pt/Pd conductive layer.

The functional groups in the poly(aryl cyanurate) layer were analyzed by means of FTIR. A PerkinElmer Spectrum Two FTIR spectrometer was used in attenuated total reflection (ATR) mode. Spectra were collected from 32 scans with a resolution of 4 cm^{-1} over a wavelength range from 450−4000 cm^{-1}. Membranes were dried prior to use and pressed on the crystal without any further preparation.

2.4. Membrane Performance. The performance of the membranes was assessed by means of pure water permeance, salt retention, MWCO, and long-term pH stability tests.

2.4.1. Pure Water Permeance. The performance of the membranes was firstly tested by means of pure water flux measurements at room temperature. For this, a custom-built dead-end filtration setup was used (Convergence B.V., the Netherlands) with an effective membrane surface area of 52.7 cm^2. Prior to each measurement, the membrane was pressurized and conditioned for 1 h at 10 bar. Subsequently, the flux at 10, 11, 13, and 15 bar was measured.

Permeance was calculated using eq 1

$$P = \frac{V}{A \times t \times \Delta p} \tag{1}$$

Here, P is the permeance ($L{\cdot}m^{-2}\ h^{-1}\ bar^{-1}$), V is the permeate volume (L), A is the membrane area (m^2), t the permeation time (h), and Δp the trans-membrane pressure (bar).

All measurements were performed on five different membrane samples ($N = 5$), which were fabricated separately using the same procedure. The error bars represent the 95% confidence interval.

2.4.2. Salt Retention. Second, salt retention measurements were performed on a custom-built setup with an effective membrane surface area of 7.548 cm^2. The membrane coupon was supported by a porous stainless-steel disk and placed at the bottom of a stainless-steel feed vessel. The vessel was filled with the feed solution, pressurized to 10 bar with nitrogen gas and stirred with an overhead stirrer at 500 rpm in order to minimize concentration polarization. The system was operated for 60 min to stabilize the conditions. After 60 min, 10 mL samples were collected for characterization.

The salt retention of the membranes was evaluated using 2 $g{\cdot}L^{-1}$ solutions of $MgSO_4$, $MgCl_2$, Na_2SO_4, and NaCl. The salt concentrations in the feed, permeate, and retentate were derived from the conductivity using a 3310 conductivity meter (WTW, Germany).

Retention was calculated using the following formula

$$R = \left(1 - \frac{C_p}{C_f}\right) \times 100\% \tag{2}$$

where R is the retention, C_f is the solute concentration in the feed, and C_p the concentration in the permeate.

Each data point represents an average of three different membrane samples ($N = 3$), error bars depict the 95% confidence interval.

2.4.3. Molecular Weight Cutoff. In order to determine the MWCO, filtration experiments with an aqueous solution of PEGs were performed. For this, the same setup and method were used as for the salt retention measurements (Section 2.4.2).

A mixture of PEGs with mean molecular weights of 200, 400, 600, 1000, and 1500 $g{\cdot}mol^{-1}$ was used, all at a concentration of 1 $g{\cdot}L^{-1}$. The compositions of the feed, the permeate, and the retentate were determined using gel permeation chromatography (GPC, Agilent Technologies 1200/1260 Infinity GPC/SEC series) according to a previously described protocol.[23] The PEG retention was then calculated using eq 2 and the MWCO was determined as the molar mass that is retained for 90% or more. Also here, three samples were tested ($N = 3$) and the 95% confidence interval was calculated.

2.5. Long-Term pH Stability Experiments. Finally, the stability of the membranes under various pH conditions was determined ex situ. Membrane coupons were exposed to a solution of either 0.1 M HNO_3 (pH 1), 0.01 M NaOH (pH 12), or 0.1 M NaOH (pH 13). After exposure for a certain time, the coupon was rinsed with Milli-Q water and salt retention measurements were performed as described in 2.4.2. The coupon was placed back in the pH solution after measurement, and after a set time this procedure was repeated. Both the permeance and retention were evaluated over time. Also, the MWCO after a long-term (>2 months) exposure was determined. Each data point is the average of three membrane coupons ($N = 3$), with error bars representing the 95% confidence interval.

https://doi.org/10.1021/acsapm.0c01366
ACS Appl. Polym. Mater. 2021, 3, 2385−2392

3. RESULTS AND DISCUSSION

The first part of the results and discussion section briefly discusses the formation of poly(aryl cyanurate) membranes and then focuses on the characterization of the TFC membranes, to verify if the poly(aryl cyanurate) film has formed. The second part focuses on the performance characterization of the produced membranes, and finally on the pH stability of these TFC membranes over time.

3.1. Fabrication and Characterization of the Poly(aryl cyanurate) Membranes. Poly(aryl cyanurate) membranes were formed by interfacial polymerization between CC in *n*-hexane and TPE, deprotonated with NaOH, in water. The phenolate anions are much more nucleophilic than the corresponding phenol moieties and readily attack the electron-deficient carbon atoms of the CC rings, displacing the chlorine atoms in a nucleophilic aromatic substitution process.[24] It is interesting to note that the reactivity of CC decreases with every chlorine atom that is displaced.[24] The mechanism of this nucleophilic aromatic substitution process is discussed later in more detail as it also applies to the base-catalyzed hydrolysis of the formed poly(aryl cyanurate) membranes.

In Figure 1, FE-SEM pictures of the support and the TFC membrane are shown. The PES support is an ultrafiltration membrane and pores are visible on the image taken of the surface (Figure 1A). Figure 1B was taken after interfacial polymerization and shows no visible pores anymore, indicating that a thin film is formed on top of the PES support. The surface morphology appears quite homogeneous, and the small cracks that are visible are the result of sample drying.

A cross-sectional image of the TFC membranes was also captured, to provide an estimate regarding the thickness of the formed layer. Figure 1C shows the presence of a thin layer on top of the support, with a thickness of approximately 100 nm with a variation in the thickness of the IP layer across the membrane of approximately ±20 nm.

The FE-SEM images indicate the formation of a thin, dense IP layer. To further characterize the formed layer and confirm the presence of the poly(aryl cyanurate) network, FTIR was performed. Figure 2 shows the transmittance data for both the

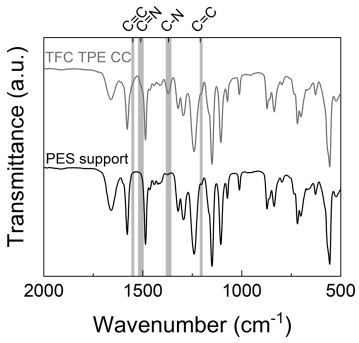

Figure 2. FTIR spectra of the PES support and the TFC TPE-CC membrane.

PES support and the TFC TPE-CC membrane. Although the majority of the peaks can be related to the PES support, there are four peaks that are distinct for the TFC membrane. The peaks at 1370 and 1505 cm^{-1} can be attributed to C−N and C═N stretching of the triazine ring. Furthermore, peaks at 1550 and 1210 cm^{-1} indicate aromatic C═C stretching, originating from TPE aromatic rings.

The analysis showed that the thin TPE-CC layer on a PES support was successfully prepared and characterized. The next step was to verify the performance in the NF regime. For this, the performance of the TPC-CC TFC membrane is analyzed in terms of pure water flux, salt retention, and MWCO.

3.2. NF Performance. Figure 3 shows the pure water flux of the TPE-CC membranes as a function of pressure. The

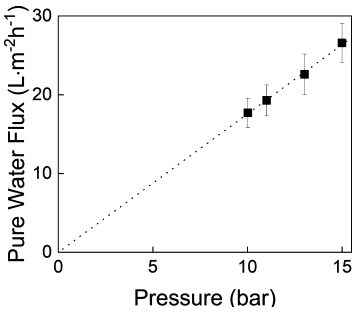

Figure 3. Pure water flux of TPE-CC membranes (*y*-axis) at different pressures (*x*-axis).

resulting linear fit indicates that no significant compaction or swelling takes place during the measurements. The average pure water permeance, for five samples, at 10 bar, is 1.77 $L{\cdot}m^{-2}$ h^{-1} bar^{-1} with a 95% CI ± 0.18 $L{\cdot}m^{-2}$ h^{-1} bar^{-1}. This is a substantial reduction compared to the pure water permeance of the support of 90 $L{\cdot}m^{-2}$ h^{-1} bar^{-1} and, therefore, also confirms the formation of a dense top layer on the support. The achieved pure water permeance is moderate when compared to other IP NF membranes (e.g., Lee et al.[11] found a permeance of 0.9 $L{\cdot}m^{-2}$ h^{-1} bar^{-1} for their polyethyleneimine-CC membranes, whereas commercial NF270 membranes[25] have a permeance as high as 13 $L{\cdot}m^{-2}$ h^{-1} bar^{-1}).

Salt retention measurements give an insight into the performance of membranes, specifically on retaining charged molecules. In Figure 4A, the salt retention is shown for four different salts. The retention decreases in the order Na_2SO_4 (97.1 ± 8.0%) > $MgSO_4$ (92.8 ± 12.7%) > NaCl (51.3 ± 4.3%) > $MgCl_2$ (32.1 ± 6.6%), which reflects the typical behavior of a negatively charged membrane. A negative surface charge of the membranes may be due to the presence of unreacted TPE phenolate anions in the network, and to anions of hydroxytriazines and triazinediols, resulting from the hydrolysis of monochloro- and dichlorotriazine moieties of the membranes. The higher retention for divalent sulfate anions (SO_4^{2-}), compared to monovalent Cl^- anions, is typical for the so-called Donnan exclusion effect.[26,27] The relatively high error bars are the result of spread within the three samples, indicating that although the same preparation method was used, some deviation in the performance exists.

Furthermore, MWCO experiments were performed to gain insights into the retention of neutral molecules, or in other words, the separation by size. The results of the MWCO experiments are summarized in Figure 4B. The PEG retention was measured for five different molecular weights as indicated by the squares, the dotted line is a guide to the eye. The MWCO (molar mass at which 90% of the PEG is retained), was found to be 400 ± 83 $g{\cdot}mol^{-1}$. Nanofiltration membranes typically have a MWCO smaller than 1000 $g{\cdot}mol^{-1}$ and,

https://doi.org/10.1021/acsapm.0c01366
ACS Appl. Polym. Mater. 2021, 3, 2385−2392

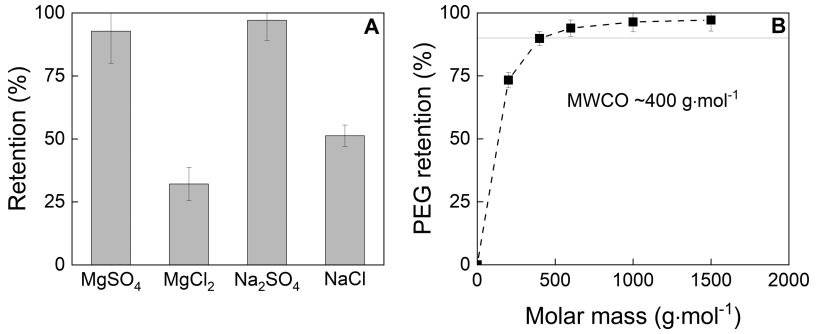

Figure 4. (A) Salt retention for four different salts. (B) PEG retention for PEGs with different molar mass. Both measured at 10 bar.

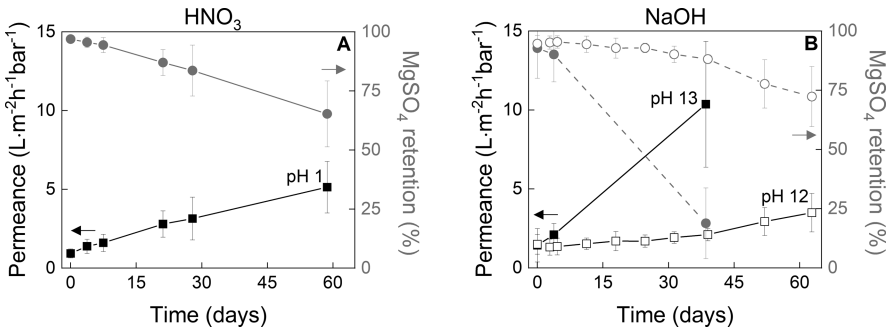

Figure 5. Permeance (left *y*-axis, black squares) and retention (right *y*-axis, gray circles) vs exposure time after exposure to (A) 0.1 M HNO_3 and (B) 0.01 (open symbols) and 0.1 M NaOH (closed symbols).

therefore, the TPE-CC membranes are well within the NF regime.

In summary, the TPE-CC membranes show performance well within the NF range, with a pure water permeance of 1.77 ± 0.18 $L{\cdot}m^{-2}\ h^{-1}\ bar^{-1}$, high salt retentions for sodium sulfate (97.1 ± 8.0%) and magnesium sulfate (92.8 ± 12.7%), and a MWCO of 400 ± 83 $g{\cdot}mol^{-1}$.

3.3. pH Stability. Figure 5 depicts the permeance and $MgSO_4$ retention after exposure to either a nitric acid (pH 1) or a sodium hydroxide (pH 12 or 13) solution for a given time.

Long-term exposure to 0.1 M HNO_3 (pH 1) is accompanied by a decrease in performance that is evident from the practically linear increase in permeance (+453%) and almost linear reduction in retention (−33%) over the course of 2 month exposure (Figure 5A). Even more severe negative trends are observed after exposure to 0.1 M NaOH (pH 13), as is shown in Figure 5B; a decrease in retention of 80% and an increase in the permeance of 620% were observed after more than 1 month exposure.

Besides exposure to 0.1 M NaOH, the membranes were also exposed to 0.01 M NaOH (pH 12), to see if the membranes would be stable under slightly less extreme conditions. Despite the fact that the performance seems to be largely stable during the first 14 days of operation, after this the degradation sets in as well. After 2 month exposure to pH 12, the retention decreased by 14% and the permeance increased to 237% of its original value.

In short, TPE-CC membranes showed a performance loss when exposed to extreme pH conditions. The degree of performance loss was also evident from MWCO experiments. Table 1 provides the MWCO before and after exposure to HNO_3 (pH 1) and NaOH (pH 12 or pH 13), respectively. After alkaline exposure, both MWCO values exceed the maximum measurable value (for our experiment) of 1500 $g{\cdot}mol^{-1}$, indicating that the NF performance is lost. In contrast, for membranes exposed to pH 1, the MWCO was between 563 and 824 $g{\cdot}mol^{-1}$, still in the NF regime and implies that the layers are not completely removed. The degradation kinetics for acidic conditions also appear to be slower compared to alkaline conditions.

Table 1. MWCO of TPE-CC Membranes after pH Exposure

before	after pH 1	after pH 12	after pH 13
401 ± 83	#1: 563, #2: 730, #3: 824[a]	>1500	>1500

[a]Sample #1 was measured immediately after finishing the pH experiments, and samples #2 and #3 were stored in Milli Q water in the fridge and were tested 5 months later.

The increase in MWCO after treatment at pH 1 is monotonic with time; even after 5 months of storage in Milli Q water, in the fridge, the MWCO increased. This indicates that, even under these conditions, the degradation continues due to the presence of (trace) acid left in the material.

The FE-SEM images in Figure 6 show the surface of the membranes before and after exposure to extreme pH conditions. From this, a better understanding can be obtained on how the morphology of the membranes is affected.

The most prevalent change is observed in Figure 6C. After exposure to pH 12 the surface is covered with "pores", which can indicate that at those spots the layer is removed. Interestingly, this same morphology is not observed for pH 13; the reason for this difference is not clear. The morphology in Figure 6D is less homogenous than before pH exposure (Figure 6A), but there are no pores visible yet. From the loss in performance a more pronounced change in morphology would have been expected.

The surface of TPE-CC membranes after pH 1 exposure does show a rougher surface (Figure 6B) compared to the original membrane. However, no clear pores or damage are

https://doi.org/10.1021/acsapm.0c01366
ACS Appl. Polym. Mater. 2021, 3, 2385−2392

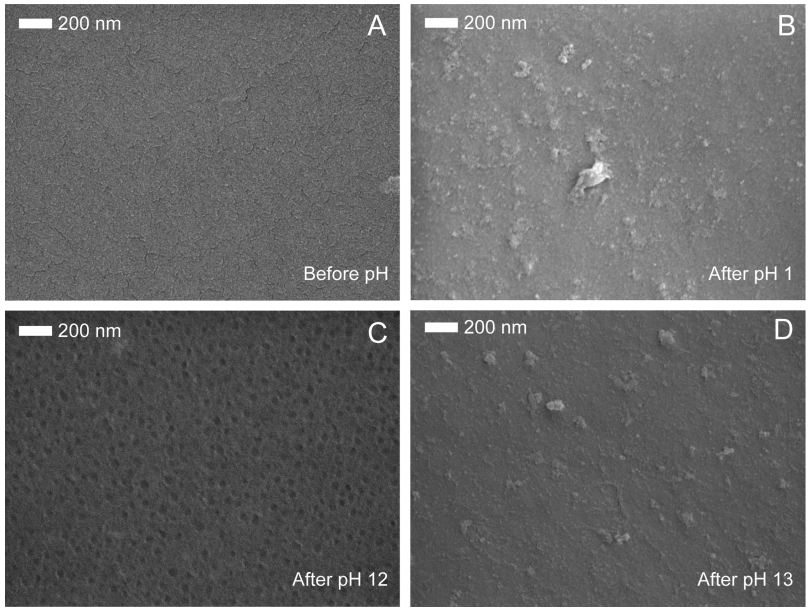

Figure 6. SEM images of TFC membranes (A) before pH exposure, (B) after pH 1, (C) after pH 12, and (D) after pH 13.

Scheme 2. Schematic Representation of Base-Catalyzed Hydrolysis of Poly(aryl cyanurate) via Nucleophilic Aromatic Substitution[a]

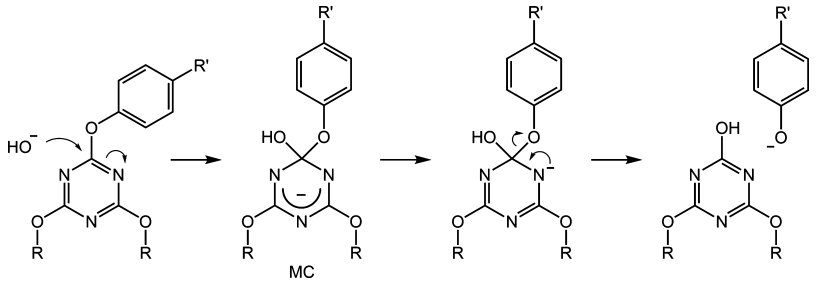

[a]The Meisenheimer complex is indicated as MC.

visible, which indicates a loss of the selective layer, as was also indicated by the MWCO tests. It must be noted that it is possible that the degradation at this point is not yet visible on the SEM images. This, however, does not mean that there is no degradation, as sub-nm damage can already be enough to affect the separation performance.

Despite the combination of aromatic rings and usually stable ether bonds, the network does show degradation upon exposure at extreme pH. This degradation can be explained by the fact that in this case, instead of normal ether bonds, aryl cyanurate type bonds are formed. Alkyl and aryl cyanurate bonds display reactivities similar to those of esters, meaning that, under the influence of pH alterations, bonds are hydrolyzed into cyanuric acid and the starting alcohol.[28,29] In Scheme 2, a schematic representation is given that indicates how the base-catalyzed hydrolysis of poly(aryl cyanurate) can take place. The electron-deficient carbon atoms of the triazine ring allow for nucleophilic attack by OH^-.[24,30] The intermediate generally postulated to result from nucleophilic attack at these nitrogen-containing heterocycles features a negative charge that is delocalized over the three nitrogen atoms of the triazine ring. In general, the anionic adduct formed when a nucleophile attacks an arene bearing electron-withdrawing groups is known as a Meisenheimer complex.[31,32] These adducts, resulting from nucleophilic aromatic substitution reactions, may be reactive intermediates but in some cases have also been isolated.[33] As the leaving group departs, aromaticity of the triazine is restored. The cyanuric acid product is hydrolytically unstable and may also degrade further into CO_2 and NH_3.[29,34]

The degradation of the TPE-CC network is confirmed by the FTIR data in Figure 7, in which after pH exposure, the distinctive peak at 1370 cm^{-1} of the C−N bond diminishes, especially for pH = 13 and pH = 12.

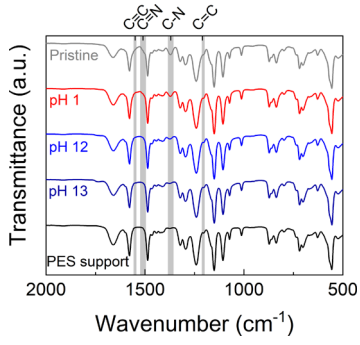

Figure 7. FTIR spectra of TFC membranes before and after pH exposure.

https://doi.org/10.1021/acsapm.0c01366
ACS Appl. Polym. Mater. 2021, 3, 2385−2392

Our results imply that the preparation of membranes from the reaction of CC with a phenol will generally not result in the exceptional high pH stability of their amine-based counterparts. The ether bonds in the aromatic network actually behave like ester bonds, which renders the network to be much more susceptible to hydrolysis.

4. CONCLUSIONS

A new type of poly(aryl cyanurate) TFC membrane was prepared via the interfacial polymerization between 1,1,1-tris(4-hydroxyphenyl)ethane and CC. ATR−FTIR and SEM confirm the formation of the network atop the PES support, in the form of a film with a thickness of ∼104 nm. The membranes prepared under the chosen experimental conditions (1 w/v % TPE, 0.01 w/v % CC, and a 30 s reaction time) exhibit nanofiltration performance with an average pure water permeance of 1.77 ± 0.18 $L{\cdot}m^{-2}\ h^{-1}\ bar^{-1}$, a MWCO of 400 ± 83 $g{\cdot}mol^{-1}$, and salt rejection follows the order: Na_2SO_4 (97.1%) > $MgSO_4$ (92.8%) > NaCl (51.3%) > $MgCl_2$ (32.1%). The salt retention is indicative of a negative surface charge.

This work was inspired by the high pH stability of polyamine membranes that originate from the reaction between CC and an aliphatic amine. By changing the amines for a phenol-based monomer, all-aromatic ether networks are obtained. The pH stability of these poly(aryl cyanurate) networks falls short of expectations, in particular at extremely high pH. This is attributed to the nature of the aryl cyanurate bonds, which act as hydrolysis-susceptible ester bonds.

■ ASSOCIATED CONTENT

Supporting Information

The Supporting Information is available free of charge at https://pubs.acs.org/doi/10.1021/acsapm.0c01366.

Interfacial polymerization setup (PDF)

■ AUTHOR INFORMATION

Corresponding Author

Nieck E. Benes − *Films in Fluids Group—Membrane Science and Technology Cluster, University of Twente, 7500 AE Enschede, The Netherlands;* orcid.org/0000-0001-9716-069X; Email: n.e.benes@utwente.nl

Authors

Maria G. Elshof − *Films in Fluids Group—Membrane Science and Technology Cluster, University of Twente, 7500 AE Enschede, The Netherlands;* orcid.org/0000-0002-4038-1413

Evelien Maaskant − *Films in Fluids Group—Membrane Science and Technology Cluster, University of Twente, 7500 AE Enschede, The Netherlands;* orcid.org/0000-0003-4691-7538

Mark A. Hempenius − *Sustainable Polymer Chemistry, Faculty of Science and Technology, MESA+, Institute for Nanotechnology, University of Twente, 7500 AE Enschede, The Netherlands*

Complete contact information is available at: https://pubs.acs.org/10.1021/acsapm.0c01366

Notes

The authors declare no competing financial interest.

■ ACKNOWLEDGMENTS

This work was funded by the Dutch Research Council (NWO): ⟨14631⟩. The authors would like to thank Bob J. Siemerink for his help with FE-SEM imaging.

■ REFERENCES

(1) Afonso, M. D.; Yañez, R. B. Nanofiltration of Wastewater from the Fishmeal Industry. *Desalination* **2001**, *139*, 429.

(2) Rautenbach, R.; Linn, T. High-pressure reverse osmosis and nanofiltration, a "zero discharge" process combination for the treatment of waste water with severe fouling/scaling potential. *Desalination* **1996**, *105*, 63−70.

(3) Luo, J.; Wan, Y. Effects of pH and salt on nanofiltration-a critical review. *J. Membr. Sci.* **2013**, *438*, 18−28.

(4) Chollom, M.; Rathilal, S.; Pillay, V.; Alfa, D. The Applicability of Nanofiltration for the Treatment and Reuse of Textile Reactive Dye Effluent. *Water SA* **2015**, *41*, 398.

(5) Tang, C.; Chen, V. Nanofiltration of Textile Wastewater for Water Reuse. *Desalination* **2002**, *143*, 11−20.

(6) Bes-Piá, A.; Mendoza-Roca, J. A.; Roig-Alcover, L.; Iborra-Clar, A.; Iborra-Clar, M. I.; Alcaina-Miranda, M. I. Comparison between Nanofiltration and Ozonation of Biologically Treated Textile Wastewater for Its Reuse in the Industry. *Desalination* **2003**, *157*, 81−86.

(7) Schaep, J.; Van Der Bruggen, B.; Uytterhoeven, S.; Croux, R.; Vandecasteele, C.; Wilms, D.; Van Houtte, E.; Vanlerberghe, F. Removal of Hardness from Groundwater by Nanofiltration. *Desalination* **1998**, *119*, 295−301.

(8) Patterson, C.; Anderson, A.; Sinha, R.; Muhammad, N.; Pearson, D. Nanofiltration Membranes for Removal of Color and Pathogens in Small Public Drinking Water Sources. *J. Environ. Eng.* **2012**, *138*, 48−57.

(9) Shao, L.; Cheng, X. Q.; Liu, Y.; Quan, S.; Ma, J.; Zhao, S. Z.; Wang, K. Y. Newly Developed Nanofiltration (NF) Composite Membranes by Interfacial Polymerization for Safranin O and Aniline Blue Removal. *J. Membr. Sci.* **2013**, *430*, 96−105.

(10) Mohammad, A. W.; Teow, Y. H.; Ang, W. L.; Chung, Y. T.; Oatley-Radcliffe, D. L.; Hilal, N. Nanofiltration Membranes Review: Recent Advances and Future Prospects. *Desalination* **2015**, *356*, 226−254.

(11) Lee, K. P.; Zheng, J.; Bargeman, G.; Kemperman, A. J. B.; Benes, N. E. PH Stable Thin Film Composite Polyamine Nanofiltration Membranes by Interfacial Polymerisation. *J. Membr. Sci.* **2015**, *478*, 75−84.

(12) Platt, S.; Nyström, M.; Bottino, A.; Capannelli, G. Stability of NF Membranes under Extreme Acidic Conditions. *J. Membr. Sci.* **2004**, *239*, 91−103.

(13) Visser, T. J. K.; Modise, S. J.; Krieg, H. M.; Keizer, K. The Removal of Acid Sulphate Pollution by Nanofiltration. *Desalination* **2001**, *140*, 79−86.

(14) Nyström, M.; Kaipia, L.; Luque, S. Fouling and Retention of Nanofiltration Membranes. *J. Membr. Sci.* **1995**, *98*, 249−262.

(15) Bes-Piá, A.; Iborra-Clar, M. I.; Iborra-Clar, A.; Mendoza-Roca, J. A.; Cuartas-Uribe, B.; Alcaina-Miranda, M. I. Nanofiltration of Textile Industry Wastewater Using a Physicochemical Process as a Pre-Treatment. *Desalination* **2005**, *178*, 343−349.

(16) Yao, C. W.; Burford, R. P.; Fane, A. G.; Fell, C. J. D.; McDonogh, R. M. Hydrolysis and Other Phenomena Affecting Structure and Performance of Polyamide 6 Membrane. *J. Appl. Polym. Sci.* **1987**, *34*, 2399−2408.

(17) Xie, Q.; Zhang, S.; Xiao, Z.; Hu, X.; Hong, Z.; Yi, R.; Shao, W.; Wang, Q. Preparation and Characterization of Novel Alkali-Resistant Nanofiltration Membranes with Enhanced Permeation and Antifouling Properties: The Effects of Functionalized Graphene Nanosheets. *RSC Adv.* **2017**, *7*, 18755−18764.

(18) Daems, N.; Milis, S.; Verbeke, R.; Szymczyk, A.; Pescarmona, P. P.; Vankelecom, I. F. J. High-Performance Membranes with Full PH-Stability. *RSC Adv.* **2018**, *8*, 8813−8827.

(19) Dalwani, M.; Bargeman, G.; Hosseiny, S. S.; Boerrigter, M.; Wessling, M.; Benes, N. E. Sulfonated Poly(Ether Ether Ketone) Based Composite Membranes for Nanofiltration of Acidic and Alkaline Media. *J. Membr. Sci.* **2011**, *381*, 81−89.
(20) Zeng, Y.; Wang, L.; Zhang, L.; Yu, J. Q. An Acid Resistant Nanofiltration Membrane Prepared from a Precursor of Poly(s-Triazine-Amine) by Interfacial Polymerization. *J. Membr. Sci.* **2018**, *546*, 225−233.
(21) Lee, K. P.; Bargeman, G.; de Rooij, R.; Kemperman, A. J. B.; Benes, N. E. Interfacial Polymerization of Cyanuric Chloride and Monomeric Amines: PH Resistant Thin Film Composite Polyamine Nanofiltration Membranes. *J. Membr. Sci.* **2017**, *523*, 487−496.
(22) Maaskant, E. Mix and match : new monomers for interfacial polymerization, **2018**. DOI: 10.3990/1.9789036545167.
(23) Elshof, M. G.; de Vos, W. M.; de Grooth, J.; Benes, N. E. On the Long-Term PH Stability of Polyelectrolyte Multilayer Nanofiltration Membranes. *J. Membr. Sci.* **2020**, *615*, 118532.
(24) Sharma, A.; El-Faham, A.; de la Torre, B. G.; Albericio, F. Exploring the Orthogonal Chemoselectivity of 2,4,6-Trichloro-1,3,5-Triazine (TCT) as a Trifunctional Linker With Different Nucleophiles: Rules of the Game. *Front. Chem.* **2018**, *6*, 516.
(25) Tanninen, J.; Mänttäri, M.; Nyström, M. Effect of Salt Mixture Concentration on Fractionation with NF Membranes. *J. Membr. Sci.* **2006**, *283*, 57−64.
(26) Peeters, J. M. M.; Boom, J. P.; Mulder, M. H. V.; Strathmann, H. Retention Measurements of Nanofiltration Membranes with Electrolyte Solutions. *J. Membr. Sci.* **1998**, *145*, 199.
(27) Schaep, J.; Van Der Bruggen, B.; Vandecasteele, C.; Wilms, D. Influence of Ion Size and Charge in Nanofiltration. *Sep. Purif. Technol.* **1998**, *14*, 155−162.
(28) Quirke, J. M. E. 1,3,5-Triazines. In *Comprehensive Heterocyclic Chemistry*; Elsevier Inc., 1984; Vol. 3−7, pp 457−530.
(29) Marella, V. V.; Throckmorton, J. A.; Palmese, G. R. Hydrolytic Degradation of Highly Crosslinked Polyaromatic Cyanate Ester Resins. *Polym. Degrad. Stab.* **2014**, *104*, 104−111.
(30) Grundmann, C. Syntheses withs-Triazine. *Angew. Chem., Int. Ed.* **1963**, *2*, 309−323.
(31) Renfrew, A. H. M.; Taylor, J. A.; Whitmore, J. M. J.; Williams, A. Nucleophilic Aromatic Substitution in Heterocycles: Alcoholysis and Hydrolysis of 2-Anilino-4,6-Dichloro-1,3,5-Triazines. *J. Chem. Soc., Perkin Trans. 2* **1994**, 2389−2393.
(32) Ormazábal-Toledo, R.; Richter, S.; Robles-Navarro, A.; Maulén, B.; Matute, R. A.; Gallardo-Fuentes, S. Meisenheimer Complexes as Hidden Intermediates in the Aza-SNAr Mechanism. *Org. Biomol. Chem.* **2020**, *18*, 4238−4247.
(33) Artamkina, G. A.; Egorov, M. P.; Beletskaya, I. P. Some aspects of anionic .sigma.-complexes. *Chem. Rev.* **1982**, *82*, 427−459.
(34) Korshak, V. V.; Gribkova, P. N.; Dmitrenko, A. V.; Puchin, A. G.; Pankratov, V. A.; Vinogradova, S. V. Thermal and Thermal-Oxidative Degradation of Polycyanates. *Polym. Sci.* **1974**, *16*, 15−23.

https://doi.org/10.1021/acsapm.0c01366
ACS Appl. Polym. Mater. 2021, 3, 2385−2392